Journal of Inflammation Research

Dovepress
open access to scientific and medical research

Open Access Full Text Article

ORIGINAL RESEARCH

Low intracellular ATP levels exacerbate carcinogen-induced inflammatory stress response and inhibit in vitro tubulogenesis in human brain endothelial cells

This article was published in the following Dove Press journal:
Journal of Inflammation Research
6 January 2011
Number of times this article has been viewed

Elizabeth Tahanian
Sabrina Peiro
Borhane Annabi

Laboratoire d'Oncologie Moléculaire, Centre de Recherche BioMED, Département de Chimie, Université du Québec à Montréal, Montréal, Québec, Canada

Abstract: Solid tumor development requires angiogenesis and is correlated to the expression of inflammatory markers through cellular metabolic and energetic adaptation. While high glycolysis rates enable the cancer cell compartment to generate adenosine triphosphate (ATP), very little is known about the impact of low intracellular ATP concentrations within the vascular endothelial cell compartment, which is responsible for tumor angiogenesis. Here, we investigated the effect of 2-deoxy-D-glucose (2-DG), a glucose analog that inhibits glycolysis through intracellular ATP depletion, on human brain microvascular endothelial cell (HBMEC) angiogenic properties. While preformed capillaries remained unaffected, we found that in vitro tubulogenesis was dose-dependently decreased by 2-DG and that this correlated with reduced intracellular ATP levels. Procarcinogenic signaling was induced with phorbol 12-myristate 13-acetate (PMA) and found to trigger the proinflammatory marker cyclooxygenase-2 (COX-2) and endoplasmic reticulum (ER) stress marker GRP78 expression, whose inductions were potentiated when PMA was combined with 2-DG treatment. Inversely, PMA-induced matrix-metalloproteinase-9 (MMP-9) gene expression and protein secretion were abrogated in the presence of 2-DG, and this can be partially explained by reduced nuclear factor-κB signaling. Collectively, we provide evidence for an intracellular ATP requirement in order for tubulogenesis to occur, and we link increases in ER stress to inflammation. A better understanding of the metabolic adaptations of the vascular endothelial cells that mediate tumor vascularization will help the development of new drugs and therapies.

Keywords: endoplasmic reticulum stress, MMP-9, COX-2, 2-deoxy-D-glucose, endothelial cells

Introduction

Tumor-associated angiogenesis, a fundamental process in tumor growth and metastasis, consists of recruiting endothelial cells (EC) toward an angiogenic stimulus.[1] The cells subsequently proliferate and differentiate to form endothelial tubes and capillary-like structures in order to deliver nutrients and oxygen to the tumor and to remove the products of its metabolism. In recent years several pathways have, in addition to stimulation of tumor angiogenesis, been suggested to contribute to the cell metabolic adaptations required for carcinogenesis, which include decreased tumoral apoptosis, increased invasion and metastasis, immune suppression, and tumor-associated inflammation.[2,3]

An interesting link between overexpression of the pro-inflammatory marker cyclooxygenase-2 (COX-2) and tumor angiogenesis was recently described as one

Correspondence: Borhane Annabi
Université du Québec à Montréal, Département de Chimie, CP 8888, Succ Centre-ville, Montréal, Québec, Canada, H3C 3P8
Tel +1 514 987 3000
Fax +1 514 987 0246
Email annabi.borhane@uqam.ca

submit your manuscript | www.dovepress.com
Dovepress
DOI: 10.2147/JIR.S15880

such metabolic adaptative phenotype.[4–6] This is supported by the fact that in normal cerebral cortex COX-2 is only present in neurons but absent from vascular EC.[7,8] It is however still unknown whether the EC-associated COX-2 correlates with high malignancy. Furthermore, little is known about the molecular events that dictate metabolic adaptation of EC in response to procarcinogenic stimuli. It is tempting to suggest that specific inhibition of metabolic pathways may offer a novel therapeutic approach that would simultaneously inhibit tumor-induced angiogenesis and inflammatory phenotypes.[9,10]

While human brain microvascular endothelial cells (HBMEC) play an essential role as structural and functional components of the blood–brain barrier (BBB), its disruption by the brain tumor-secreted matrix metalloproteinase-9 (MMP-9) is believed to favor tumor invasion.[11,12] Recent studies delineated a unique brain endothelial phenotype in which MMP-9 secretion by HBMEC was increased upon treatment with the tumor-promoting agent phorbol 12-myristate 13-acetate (PMA).[13,14] Inhibition of MMP-9 secretion was demonstrated to reduce both in vitro invasion and angiogenesis in human microvascular EC.[15] In fact, adenoviral-mediated MMP-9 downregulation inhibited human dermal microvascular EC migration in cell wounding and spheroid migration assays, and reduced capillary-like tube formation, demonstrating the key role of MMP-9 in EC network organization.[15] Therefore, among all MMP, the MMP-9 secreted from brain EC may be of importance in brain tumor-associated neovascularization.

Among the numerous signaling pathway candidates, nuclear factor-κB (NF-κB) can regulate the expression of COX-2 through endoplasmic reticulum (ER) stress and, in part, through induction of the ER chaperone GRP78/BiP, which is expressed at high levels in a variety of tumors and which confers drug resistance to both proliferating and dormant cancer cells.[16] Importantly, it was recently demonstrated that partial reduction of GRP78 substantially reduced tumor microvessel density.[17] In the current study, we treated HBMEC with 2-deoxy-D-glucose (2-DG) which, once phosphorylated by hexokinase to 2-deoxyglucose-6-phosphate, cannot be further metabolized and leads to a blockade of glycolysis and to depletion of intracellular adenosine triphosphate (ATP). In vitro tubulogenesis, expression of ER stress marker GRP78, PMA-induced MMP-9 secretion, and COX-2 were also assessed in order to provide a metabolic and adaptative link between endothelial inflammation and angiogenesis.

Materials and methods

Materials

2-Deoxy-D-glucose, sodium dodecylsulfate (SDS) and bovine serum albumin (BSA) were purchased from Sigma-Aldrich Canada (Oakville, Canada). Electrophoresis reagents were purchased from Bio-Rad (Mississauga, Canada). The enhanced chemiluminescence (ECL) reagents were from Perkin Elmer (Waltham, MA). Micro bicinchoninic acid protein assay reagents were from Pierce (Rockford, IL). The polyclonal antibodies against IκB and phospho-IκB were purchased from Cell Signaling (Danvers, MA). The monoclonal antibodies against GRP78 and GAPDH were from Advanced Immunochemical Inc (Long Beach, CA). Horseradish peroxidase-conjugated donkey anti-rabbit and anti-mouse IgG secondary antibodies were from Jackson ImmunoResearch Laboratories (West Grove, PA). All other reagents were from Sigma-Aldrich Canada.

Cell culture

HBMEC were characterized and generously provided by Dr. Kwang Sik Kim of the Johns Hopkins University School of Medicine (Baltimore, MD). These cells were positive for factor VIII-Rag, carbonic anhydrase IV, and Ulex Europeus Agglutinin I; they took up fluorescently labeled, acetylated low-density lipoprotein and expressed gamma glutamyl transpeptidase, demonstrating their brain EC-specific phenotype.[18] HBMEC were immortalized by transfection with simian virus 40 large T antigen and maintained their morphological and functional characteristics for at least 30 passages.[19] HBMEC were maintained in RPMI 1640 (Gibco, Burlington, Canada) supplemented with 10% (v/v) heat-inactivated fetal bovine serum (iFBS) (HyClone Laboratories, Logan, UT), 10% (v/v) NuSerum (BD Bioscience, Mountain View, CA), modified Eagle's medium nonessential amino acids (1%) and vitamins (1%) (Gibco), sodium pyruvate (1 mM) and EC growth supplement (30 μg/mL). Culture flasks were coated with 0.2% type-I collagen to support the growth of HBMEC monolayers. Cells were cultured at 37°C under a humidified atmosphere containing 5% CO_2. All experiments were performed using passages 3 to 28.

Endothelial cell morphogenesis assay

Tubulogenesis was assessed using Matrigel aliquots of 50 μL, plated into individual wells of 96-well tissue culture plates (Costar, Amherst, MA) and allowed to polymerize at 37°C for 30 min. After brief trypsinization, HBMEC were washed and resuspended at a concentration of 10^6 cells/mL in serum-free medium. Twenty-five microliters of cell

suspension (25,000 cells/well) and 75 µL of medium with serum were added into each culture well. Cells were allowed to form capillary-like tubes at 37°C in 5% CO_2/95% air for 20 h in the presence or absence of different 2-DG concentrations. The formation of capillary-like structures was examined microscopically and images (100×) were recorded using a Retiga 1300 camera (QImaging, Surrey, Canada) and an Eclipse TE2000-U microscope (Nikon, Melville, NY). The extent to which capillary-like structures formed in the gel was quantified by analysis of digitized images to determine the thread length of the capillary-like network, using a commercially available image analysis program (Northern Eclipse; Empix, Mississauga, Canada) as described and validated previously.[20,21] For each experiment, four randomly chosen areas were quantified by counting the number of tubes formed. Tubulogenesis data are expressed as a mean value derived from at least three independent experiments.

Gelatin zymography

Gelatin zymography was used to assess the extent of proMMP-2 and proMMP-9 activity as described previously.[22] Briefly, an aliquot (20 µL) of the culture medium was subjected to SDS-PAGE in a gel containing 0.1 mg/mL gelatin. The gels were then incubated in 2.5% Triton X-100 and rinsed in nanopure distilled H_2O. Gels were further incubated at 37°C for 20 h in 20 mM NaCl, 5 mM $CaCl_2$, 0.02% Brij-35, 50 mM Tris-HCl buffer, pH 7.6, then stained with 0.1% Coomassie Brilliant blue R-250 and destained in 10% acetic acid, 30% methanol in H_2O. Gelatinolytic activity was detected as unstained bands on a blue background.

Immunoblotting procedures

Proteins or nuclear extracts were isolated from control and treated cells using the NE-PER Nuclear and cytoplasmic extraction kit (Pierce) and were separated by SDS–polyacrylamide gel electrophoresis (PAGE). After electrophoresis, proteins were electrotransfered to polyvinylidene difluoride membranes which were then blocked for 1 h at room temperature with 5% nonfat dry milk in Tris-buffered saline (150 mM NaCl, 20 mM Tris–HCl, pH 7.5) containing 0.3% Tween-20 (TBST). Membranes were further washed in TBST and incubated with the primary antibodies (1/1000 dilution) in TBST containing 3% bovine serum albumin, followed by a 1 h incubation with horseradish peroxidase-conjugated anti-rabbit or anti-mouse IgG (1/2,500 dilution) in TBST containing 5% nonfat dry milk. Immunoreactive material was visualized by enhanced chemiluminescence (Amersham Biosciences, Baie d'Urfée, Canada).

Analysis of cell death by flow cytometry

Cell death was assessed by flow cytometry as described previously.[23] Adherent and floating cells were harvested by trypsin digestion and gathered to produce a single cell suspension. The cells were pelleted by centrifugation and washed with phosphate-buffered saline (PBS). Then, 10^5 cells were pelleted, resuspended in 200 µL of buffer solution, and stained with annexin-V-fluorescein isothiocyanate and propidium iodide (PI) according to the manufacturer's protocol (BD Biosciences, Mississauga, Canada). The cells were diluted by adding 300 µL of buffer solution and processed for data acquisition and analysis on a Becton Dickinson FACS Calibur flow cytometer using CellQuest Pro software.

Analysis of autophagy by fluorescent microscopy and flow cytometry

HBMEC were seeded onto 12-well plates and cultured for 18 h to reach 80% confluence. Cells were then exposed to different concentrations of 2-DG in the presence or absence of PMA (1 µM) in serum-free medium at 37°C in 5% CO_2/95% air. Acridine orange was added to the culture medium at a final concentration of 0.5 µg/mL and incubated for 15 min in the dark at 37°C. The cells were then washed two times with medium lacking phenol red. Cells were immediately analyzed by flow cytometry or images taken with a fluorescent microscope using 510–560 nm for excitation and 590 nm for emission.

Intracellular ATP levels assay

Cells were treated and 10X–100X-diluted lysates kept on ice as described by the manufacturer (Sigma). One hundred microliters of ATP mix was added to the lysates and incubated at room temperature for 3 min. Somatic cell ATP-releasing reagent (1X) was prepared and added to the cell lysates. From this solution 100 µL was added to the ATP mix prior to analysis by spectrofluorimetry.

Statistical analysis

Statistical analyses were performed with Student's *t*-test when one group was compared with the control group. To compare two or more groups with the control group, one-way analysis of variance (ANOVA) with Dunnett's post hoc test was used. All statistical analyses were performed using Prism software (GraphPad, La Jolla, CA). Differences with $P < 0.05$ were considered significant.

Results

2-Deoxy-D-glucose depletes intracellular ATP and inhibits in vitro capillary-like structure formation in HBMEC

We first tested the effects of 2-DG against the angiogenic properties of HBMEC. Cells were seeded on top of Matrigel and left to adhere as described in the Methods section. Upon capillary-like structure formation, we then added 10–100 mM 2-DG or Mannose. No effect was found on the integrity of the preformed structures (Figure 1A). In contrast, when various concentrations of 2-DG were added at the very early time points (ie, 30 min after cell seeding on top of Matrigel), cell structure formation was significantly decreased with a half maximal inhibitory concentration (IC_{50}) of 4.1 mM (Figure 1B). Cell survival was assessed with annexin-V-fluorescein isothiocyanate (apoptosis) and propidium iodide (necrosis) and was not significantly affected by 2-DG (Figure 1C). Mannose did not affect the capacity of the cells to form structures (not shown). We also validated 2-DG's ability to deplete intracellular ATP levels in HBMEC. While vehicle or 2-DG treatment did not affect total protein content levels (Figure 1D), we found that intracellular ATP levels decreased by ~20% in vehicle-treated cells during the 24 h incubation prior to which tube formation was assessed (Figure 1D, left panel). When cells were treated with 100 mM 2-DG, >60% of intracellular ATP was depleted within the first hour of treatment, and >90% depletion was achieved at 4 h of treatment (Figure 1D, right panel). ATP-dependent inhibition of tubulogenesis was investigated next to find out whether any extracellular matrix (ECM) degrading events were involved in this 2-DG effect.

2-Deoxy-D-glucose inhibits PMA-induced MMP-9 secretion in HBMEC

Among the secreted enzymes involved in ECM degradation, matrix metalloproteinases (MMP) are well

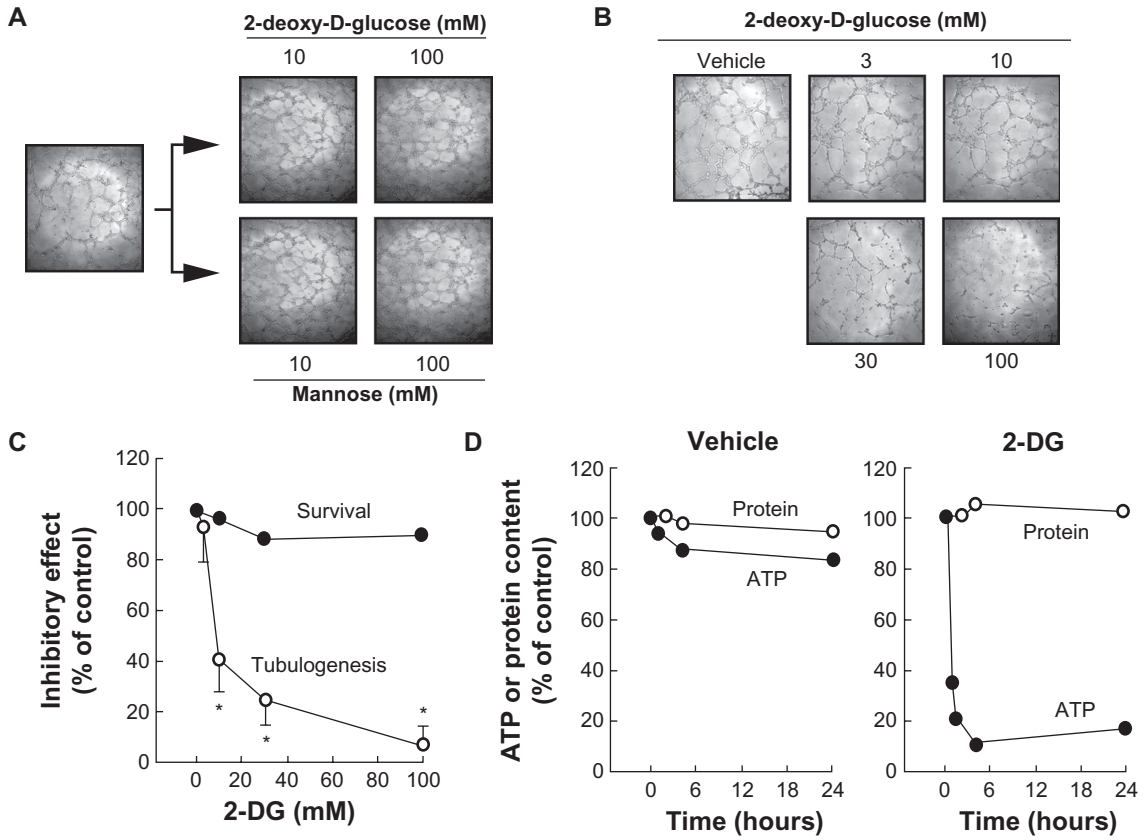

Figure 1 2-DG (mM) depletes intracellular ATP and inhibits in vitro capillary-like structure formation in HBMEC. In order to assess the impact of ATP requirement for in vitro tubulogenesis, HBMEC were seeded on top of Matrigel as described in the Methods section and left to form structures. **A**) Capillaries were then treated with 2-DG (mM) or Mannose (mM). **B**) The impact of 2-DG was also monitored during the formation of the structures, where cells were treated with various concentrations of 2-DG 30 min after seeding of the cells on top of Matrigel, and structure formation monitored after 18 h. Representative phase contrast pictures were taken. **C**) The extent of three-dimensional capillary-like structure formation (tubulogenesis) and of cell survival was assessed as described in the Methods section. **D**) Intracellular ATP as well as total protein content were assessed as described in the Methods section in vehicle- or 2-DG-treated cells. The length of the tube network was quantitated using Northern Eclipse software.
Notes: Values are means of two independent experiments (*$P < 0.01$ versus control alone); bars, ± SD.
Abbreviations: HBMEC human brain microvasular endothelial cell; ATP, adenosine triphosphate; 2-DG, 2 deopy-D-glucose.

documented as being involved in cell migration and tubulogenesis.[13,24] More specifically, MMP-2 and MMP-9 are secreted by numerous cell types and their presence is often representative of angiogenesis.[25,26] HBMEC were serum-starved, treated for 18 h with 2-DG, and the conditioned media were harvested to measure the levels of MMP-2 and of MMP-9 in both control and in PMA-treated cells by gelatin zymography. While MMP-2 extracellular levels were unaffected by 2-DG or by PMA (Figure 2A), MMP-9 levels were undetectable in basal conditions but were significantly increased in PMA-treated cells (Figure 2A, lower panel); the simultaneous presence of 2-DG significantly attenuated the MMP-9 levels seen in the presence of PMA with an IC_{50} of ~18.1 mM (Figure 2B). Collectively, these results suggest that changes in intracellular ATP levels do not inhibit MMP vesicular trafficking since MMP-2 secretion was unaffected, but do affect signal transducing events such as those triggered by PMA and which control MMP-9 secretion.

2-Deoxy-D-glucose inhibits PMA-induced IκB phosphorylation and nuclear translocation of the p65 subunit of NF-κB

Among MMP-9 expression regulators, the NF-κB signaling pathway has been suggested.[27] We therefore first assessed whether this signaling was activated upon PMA treatment and whether it was reflected in IκB degradation. PMA-mediated phosphorylation of IκB was assessed. HBMEC were treated for 45 min with 1 μM PMA following preincubation with either vehicle or with 100 mM 2-DG. Preincubation with vehicle followed by PMA treatment rapidly led to IκB phosphorylation and to a concomitant decrease in IκB (Figure 3A, upper panels). When cells were preincubated with 2-DG (Figure 3A, lower panels), PMA-mediated IκB phosphorylation was significantly reduced (Figure 3B) as quantified by scanning densitometry. Nuclear translocation of the p65 and p50 subunits of NF-κB is among the direct consequences of IκB phosphorylation. When nuclear extracts were isolated, we found that lower p65 nuclear translocation (Figure 4A) occurred when cells were treated both with PMA and 2-DG as compared to PMA alone (Figure 4B). This is in agreement with the reduced phosphorylation of IκB observed in Figure 3.

2-Deoxy-D-glucose potentiates PMA-induced cyclooxygenase-2 and GRP78 expression

As PMA is also a well documented inducer of cyclooxygenase-2 (COX-2),[28] we determined whether 2-DG also inhibited a possible NF-κB signaling pathway that leads to COX-2 induction. Cells were first treated with PMA or a combination of PMA/2-DG or PMA/Man (mannose served as an osmotic control). PMA induced COX-2 expression, which was exacerbated in PMA/2-DG-treated cells, which had increased GRP78 expression further (Figure 5A, left panel). These effects were not observed in PMA/Man-treated

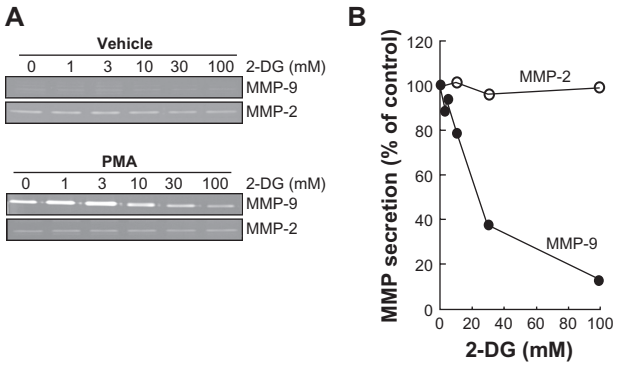

Figure 2 2-DG inhibits PMA-induced MMP-9 secretion in HBMEC. HBMEC were serum-starved in the presence of various concentrations of 2-DG in combination with vehicle or 1 μM PMA for 18 h. **A**) Conditioned media were then harvested and gelatin zymography was performed in order to detect proMMP-9 and proMMP-2 hydrolytic activity as described in the *Methods* section. **B**) Scanning densitometry was used to quantify the extent of either basal proMMP-2 gelatin hydrolysis (open circles), or proMMP-9 (closed circles) in PMA-treated cells.

Note: Data shown are representative of two independent experiments.

Abbreviations: 2-DG, 2-dexy-D-glucose; HBMEC, mitovasuila endothelial cells; MMP, matrix metalloproteinase; PMA, phorbol 12-myristate 13-acetate; GADPH, glyceraldetyde 3- phisiphate dehydrogenase; PAGE, pohyacrylanide electrophoresis.

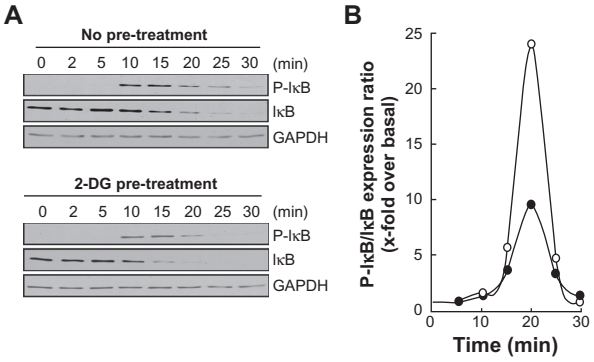

Figure 3 2-DG inhibits PMA-induced IκB phosphorylation that leads to IκB degradation. **A**) HBMEC were serum-starved for 30 min in the presence of either vehicle or 100 mM 2-DG. Cells were then incubated for the indicated time with 1 μM PMA. Lysates were isolated, electrophoresed via SDS-PAGE and immunodetection of phosphorylated IκB (P-IκB), IκB, and of GAPDH proteins was performed as described in the Methods section. **B**) Quantification was performed by scanning densitometry of the autoradiograms. Data were expressed as x-fold induction over basal untreated cells of the P-IκB/IκB ratios in vehicle pre-treated cells (open circles) and 2-DG pre-treated cells (closed circles).

Abbreviations: 2-DG, 2-dexy-D-glucose; HBMEC, mitovasuila endothelial cells; MMP, matrix metalloproteinase; PMA, phorbol 12-myristate 13-acetate; GADPH, glyceraldetyde 3- phisiphate dehydrogenase; PAGE, pohyacrylanide electrophoresis.

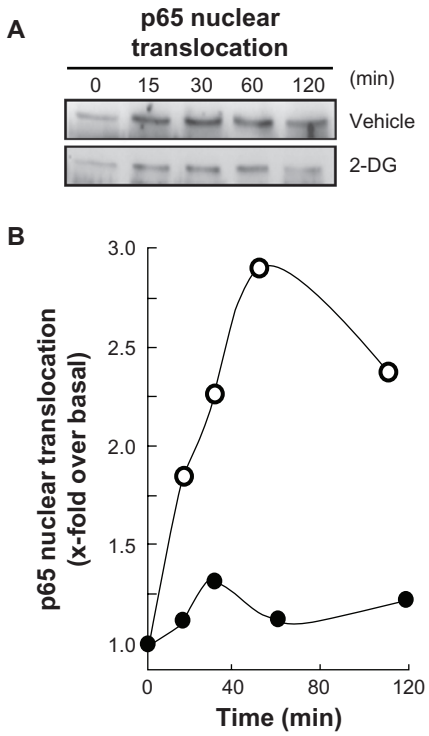

Figure 4 2-DG inhibits PMA-induced nuclear translocation of the p65 subunit of NF-κB. **A**) HBMEC were serum-starved for 30 min in the presence of either vehicle or 100 mM 2-DG. Cells were then incubated for the indicated time with 1 μM PMA. Nuclear extracts were isolated, electrophoresed via SDS-PAGE and immunodetection of the p65 subunit of NF-κB protein was performed as described in the Methods section. **B**) Quantification was performed by scanning densitometry of the autoradiograms. Data were expressed as x-fold induction over basal untreated cells of the vehicle pretreated cells (open circles) and 2-DG pre-treated cells (closed circles).

Abbreviations: HBMEC, mitovasuila endothelial cells; PAGE, pohyacrylanide electrophoresis. PMA, phorbol 12-myristate 13-acetate; 2-DG-glucose.

cells (Figure 5A, right panel). To investigate the dose-dependent effect, cells were incubated with vehicle or PMA in the presence of various 2-DG concentrations for 24 h. No COX-2 expression was observed in the absence of PMA, while a slight basal increase in the ER stress marker GRP78 was noticed with increasing 2-DG treatment (Figure 5B, left panel). As expected, COX-2 expression was significantly induced by PMA (Figure 5B, right panel), and this induction was dose-dependently potentiated by 2-DG (Figure 5C). This 2-DG-mediated potentiation is in contrast to the results seen with MMP-9 and with the reduced NF-κB signaling described above (Figure 3 and Figure 4). Interestingly, we also found that the 2-DG-mediated expression of the ER stress marker GRP78 was potentiated upon PMA treatment (Figure 5D). Altogether, our data suggest ATP depletion affects PMA-mediated signaling independent of NF-κB and results in both decreased MMP-9 levels and in increased COX-2 expression. The latter is possibly a consequence of ER stress induction.

Increased endoplasmic reticulum stress, rather than MMP-mediated ECM hydrolysis, correlates with cyclooxygenase-2 expression in HBMEC

As a consequence of the results above, we suspected a correlative relationship that would direct the molecular events observed following intracellular ATP depletion within HBMEC. Accordingly, we plotted GRP78 vs COX-2 as well as MMP-9 vs COX-2 and confirmed a positive correlation between ER stress and COX-2 expression (Figure 6A). As for MMP-9 and its possible involvement in the ECM degradation required for tubulogenesis to occur, we instead found an inverse correlation when plotted against COX-2 expression (Figure 6B). Collectively, this suggests that intracellular ATP needs are crucial for cell survival signaling through ER stress-mediated events that would lead to a proinflammatory phenotype.

2-Deoxy-D-glucose-induced autophagy is abrogated in PMA-treated HBMEC

Given that 2-DG treatment of the cells did not result in any cytotoxic effect (Figure 1B), we tested the possible implication of autophagy, a crucial component of the cellular stress adaptation response that maintains cell homeostasis and that may act as a survival mechanism that can rescue cells from apoptotic/necrotic death. HBMEC were treated in the presence of 100 mM 2-DG in combination or not with PMA. The acidic autophagic vesicles were visualized by supravital staining with a pH-sensitive dye acridine orange and fluorescent microscopy used to for visualization (Figure 7A). We observed that 2-DG, but more importantly PMA, triggered autophagic vacuoles formation which effect was slightly increased in the presence of combined 2-DG/PMA treatment. When flow cytometry was used to quantify the extent of autophagy, we found that 2-DG induced by 2.4-times autophagy (Figure 7B). PMA treatment alone triggered extensive autophagy, but when combined to 2-DG no increase (1.1-times over basal) in autophagy was observed.

Discussion

The adaptive mechanisms responsible for EC survival under pro-carcinogenic and low energy conditions remain poorly documented. Although increasing interest has been manifested towards cancer therapies that target cell metabolism, very few studies have specifically assessed the impact of targeting the EC metabolic compartment. In fact, EC are believed to be metabolically robust and to adapt to

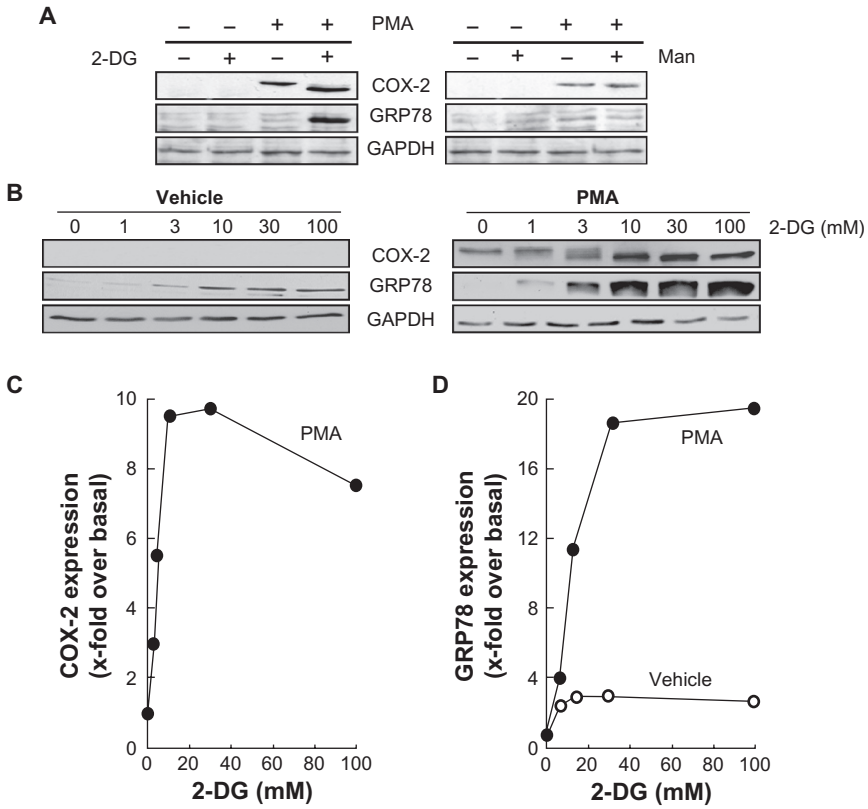

Figure 5 2-DG potentiates PMA-induced cyclooxygenase-2 and GRP78 expression. **A**) HBMEC were serum starved for 18 h in the presence or absence of 1 μM PMA and in combination with either 30 mM 2-DG or 30 mM Man. Lysates were isolated, electrophoresed via SDS-PAGE, and immunodetection of COX-2, GRP78, and GAPDH was performed as described in the *Methods* section. **B**) HBMEC were treated as in (A) with various doses of 2-DG. Lysates were isolated, electrophoresed via SDS-PAGE, and immunodetection of COX-2, GRP78, and GAPDH was performed as described in the Methods section. **C**) Scanning densitometry of COX-2 expression was only performed in PMA-treated cells since no COX-2 was detectable in vehicle-treated cells. **D**) Scanning densitometry of GRP78 expression was performed in vehicle- and in PMA-treated cells.

Abbreviations: HBMEC, mitovasuila endothelial cells; PMA, phorbol 12-myristate 13-acetate; 2-DG-glucose; PAGE, pohyacrylanide electrophoresis; GADPH, glyceraldetyde, 3-phisiphate; man, mannose.

pro-carcinogenic paracrine stimulation and conditions such as encountered within the hypoxic tumor microenvironment.[29,30] In our study, we induced in vitro procarcinogenic stimulation of brain microvascular endothelium using PMA in combination with ATP-depleting culture conditions in order to assess EC angiogenic and inflammatory responses. While preformed endothelial structures remained unaffected by 2-DG-mediated ATP depletion, we show that minimal

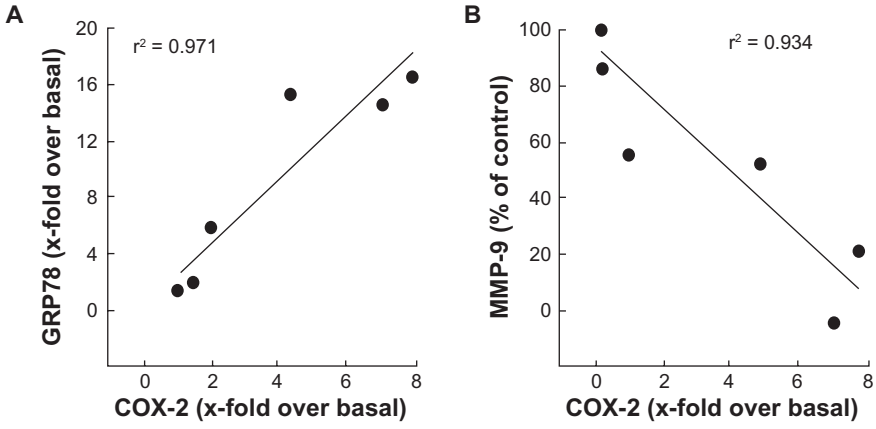

Figure 6 Increased endoplasmic reticulum stress, rather than MMP-mediated ECM hydrolysis, correlates with cyclooxygenase-2 expression in HBMEC. The effects of PMA treatments in the presence of increasing 2-DG concentrations were plotted in order to assess any correlation between **A**) ER stress (GRP78 expression) and inflammation (COX-2 expression), and **B**) between ECM hydrolysis (MMP-9 expression) and inflammation.

Abbreviations: ECM,extracellular matrix; MMP, matrix metallo prsteinase; HBMEC, mitovasuila endothelial cells; PMA, phorbol 12-myristate 13-acetate; 2-DG-glucose; ER, endoplasmic reticulam.

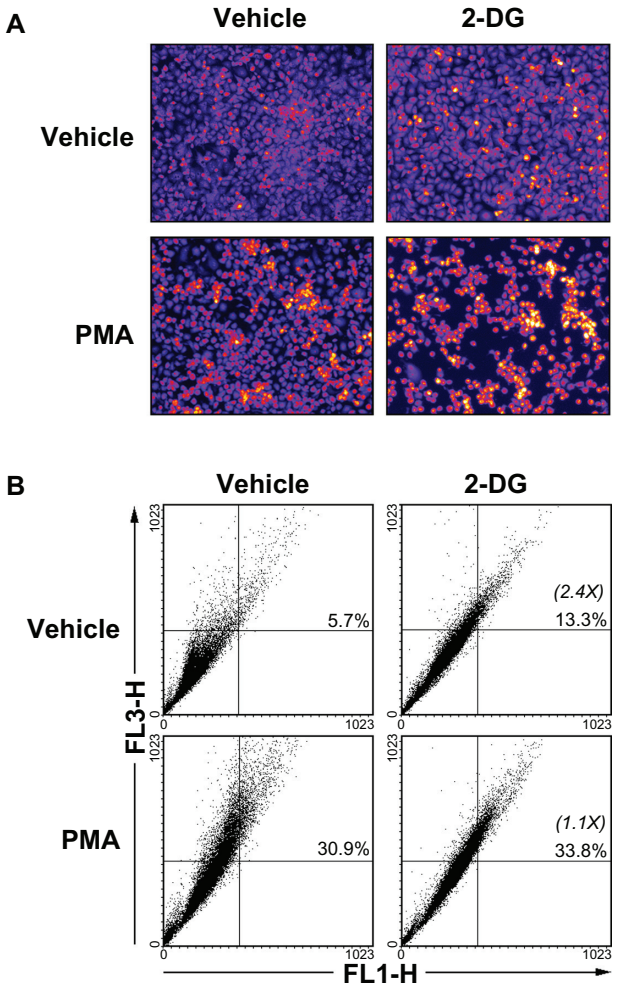

Figure 7 2-DG induced autophagy is abrogated in PMA-treated HBMEC. Autophagy was assessed as described in the Methods section in vehicle, 100 mM 2-DG-, 1 μM PMA-, and 100 mM 2-DG/1 μM PMA-treated HBMEC. **A**) Representative microphotographs of the formation of acidic vesicular organelles were taken upon acridine orange staining. **B**) The extent of autophagy was further confirmed by flow-cytometry of acridine orange stained cells and the percent of autophagy indicated for each condition. In between parenthesis, the extent of autophagy induction is indicated.
Abbreviations: HBMEC, mitovasuila endothelial cells; PMA, phorbol 12-myristate 13-acetate; 2-DG-glucose.

supply of energy is required by HBMEC for tubulogenesis processes to occur and that the acquisition of a proinflammatory phenotype better correlates with induction of ER stress than with increased ECM degradation capacities. This is among the first demonstration linking molecular players such as GRP78 (ER stress) and COX-2 (inflammation) expression to the adaptative survival mechanisms of vascular EC's response to procarcinogenic and ATP-depleting conditions. More importantly, this also in part *demonstrates* the crucial requirement for ATP in the early time points of tubulogenesis processes, while preformed vessels may adopt metabolic adaptative mechanisms enabling them to resist energy depletion. Alternate strategies, aside from using energy depletion agents, must therefore be envisioned in order to target preformed tumor-associated vessels, while optimization of antiangiogenic therapies may be complemented with ATP-depleting strategies.

EC are the first cells to be exposed to decreases in PO_2 within a hypoxic tumor-associated environment. Accordingly, tight regulation of ATP and GTP turnover exists, which enables EC to maintain their high-energy phosphates during hypoxia.[31] In EC, ATP is also predominantly generated by glycolysis and O_2 consumption is comparatively low.[29] Although accelerated glycolysis is one of the biochemical characteristics of cancer cells metabolism, one can safely extrapolate that this metabolic shift alteration, in part consequent to the hypoxic tumor microenvironment, must also occur within the tumor-associated vascular endothelium. Accordingly, it was demonstrated that low energy demand and high glycolytic activity may explain why the coronary endothelium is less severely injured than cardiomyocytes in ischemic and anoxic hearts.[29] Targeting glycolysis in the tumor-associated vascular compartment may become an attractive antiangiogenic approach. As such, besides affecting cell death and stress signaling pathways, 2-DG was recently shown to activate autophagy via ER stress rather than ATP depletion in cancer cell lines.[32] Autophagy is a crucial component of the cellular stress adaptation response that maintains mammalian homeostasis, a process believed to protect against neurodegenerative and inflammatory conditions, aging, and cancer. Similar to tumor cells defense mechanisms, one can therefore hypothesize that the ER stress consequent to 2-DG treatment in tumor-associated EC may contribute to autophagy and promote cell survival (this study). While protective effects of autophagy were observed in the cancer cell compartment in both laser-induced cell death[33] and in resveratrol-induced cytotoxicity in glioma cells,[34] inhibition of autophagy was on the other hand found to potentiate antiangiogenic effects of sulforaphane in an EC model.[35] Our study provides evidence supporting the latter assumption whereas 2-DG-mediated inhibition of autophagy was only observed in carcinogen-treated HBMEC (Figure 7B). Deployment of therapeutic strategies to block autophagy for cancer and/or antiangiogenic therapy may therefore be envisioned.

Our study documents the effects of limited intracellular ATP levels not only on the EC angiogenic properties but also on their capacity to express inflammatory markers. We showed that ATP depletion upon procarcinogenic stimulation with PMA exacerbates COX-2 expression in HBMEC, an effect correlated to ER stress-mediated mechanism. It

has been established that COX-2 is usually undetectable in normal tissues, but can be induced through several stimuli, including mitogens, growth factors, hormones, and cytokines.[36] In recent years, many molecular pathways have been proposed to explain how increased COX-2, and the resulting prostaglandin over-production, may contribute to carcinogenesis.[37] COX-2 mediates this role through the specific production of PGE_2 that acts to inhibit apoptosis, promote cell proliferation, stimulate angiogenesis, and decrease immunity.[38] To date, only few reports document an association between COX-2 expression and survival in EC consequent to tissue injury. In fact, it is believed that sepsis, consequent to the release of the endotoxin lipopolysaccharide (LPS) by Gram-negative bacteria, is regulated through induction of COX-2 expression. One can therefore envision a close parallel between proinflammatory molecular mechanisms involved in endotoxin-induced brain tissue injury and inflammation associated to brain tumor development. Interestingly, LPS-induced COX-2 expression was recently reported in bEnd.3 mouse brain endothelial cells.[39] This study actually provides strong support to our study as the contribution of NF-κB (p65) activation was reported to also regulate COX-2.[39] Noteworthy, LPS-induced adenosine was demonstrated to promote angiogenesis by the upregulation of VEGF expression in macrophages.[40] Whether such a conceptual model impacts on the link between proinflammatory COX-2 and increased tumor angiogenesis remains to be further investigated.

On the other hand, moderate activity of the ER stress response system exerts an antiapoptotic function and supports tumor cell survival and chemoresistance, whereas more severe aggravation may exceed the protective capacity of this system and turn on its proapoptotic module.[38] In our study we demonstrate in vitro, through the combination of two pharmacologic approaches, that increased COX-2 expression only occurs within those EC which possess low intracellular ATP levels and which are cultured under procarcinogenic conditions. 2-DG-mediated ATP depletion combined with PMA-induced ER stress synergize and inhibit autophagy potential of PMA-treated cells, an effect which ultimately impacts on EC angiogenic properties (ie, low tubulogenesis and diminished MMP-9 secretion). Similar cytotoxic outcome was recently documented in human breast cancer cells where the HIV protease inhibitor nelfinavir (Viracept; Agouron Pharmaceuticals Inc., La Jolla, CA) and the COX-2 inhibitor celecoxib (Celebrex; Pfizer, New York, NY) were combined and produced aggravated ER stress, which caused pronounced toxicity.[38]

In summary, the present study has demonstrated that minimal ATP is required for EC-mediated tubulogenesis to occur. Moreover, we provide evidence that combined ATP depletion and procarcinogenic signaling trigger exacerbated ER stress that leads to the acquisition of a proinflammatory phenotype as reflected by increased COX-2 induction. Altogether, the combined output of those mechanisms may further impact on the cell survival adaptative response and trigger antiangiogenic effects within the tumor-associated vascular endothelium.

Acknowledgments

BA holds a Canada Research Chair in Molecular Oncology from the Canadian Institutes of Health Research. ET is a Fonds de Recherche sur la Nature et les Technologies (FQRNT) awardee. This study was funded by a grant from the Natural Sciences and Engineering Research Council of Canada to BA.

Disclosure

The authors report no conflicts of interest in this work.

References

1. Hanahan D, Folkman J. Patterns and emerging mechanisms of the angiogenic switch during tumorigenesis. *Cell*. 1996;86:353–364.
2. Rojas A, Figueroa H, Morales E. Fueling inflammation at tumor microenvironment: the role of multiligand/RAGE axis. *Carcinogenesis*. 2010;31:334–341.
3. Hayes A. Cancer, cyclo-oxygenase and nonsteroidal anti-inflammatory drugs – can we combine all three? *Vet Comp Oncol*. 2007;5:1–13.
4. Costa C, Soares R, Reis-Filho JS, et al. Cyclo-oxygenase 2 expression is associated with angiogenesis and lymph node metastasis in human breast cancer. *J Clin Pathol*. 2002;55:429–434.
5. Fournier LS, Novikov V, Lucidi V, et al. MR monitoring of cyclooxygenase-2 inhibition of angiogenesis in a human breast cancer model in rats. *Radiology*. 2007;243:105–111.
6. Müller-Decker K, Fürstenberger G. The cyclooxygenase-2-mediated prostaglandin signaling is causally related to epithelial carcinogenesis. *Mol Carcinog*. 2007;46:705–710.
7. Breder CD, Saper CB. Expression of inducible cyclooxygenase mRNA in the mouse brain after systemic administration of bacterial lipopolysaccharide. *Brain Res*. 1996;713:64–69.
8. Yamagata K, Andreasson KI, Kaufmann WE, et al. Expression of a mitogen-inducible cyclooxygenase in brain neurons: regulation by synaptic activity and glucocorticoids. *Neuron*. 1993;11:371–386.
9. Cascante M, Boros LG, Comin-Anduix B, et al. Metabolic control analysis in drug discovery and disease. *Nat Biotechnol*. 2002;20:243–249.
10. Boros LG, Cascante M, Lee WN. Metabolic profiling of cell growth and death in cancer: applications in drug discovery. *Drug Discov Today*. 2002;7:364–372.
11. Lakka SS, Gondi CS, Rao JS. Proteases and glioma angiogenesis. *Brain Pathol*. 2005;15:327–341.
12. Bonoiu A, Mahajan SD, Ye L, et al. MMP-9 gene silencing by a quantum dot-siRNA nanoplex delivery to maintain the integrity of the blood brain barrier. *Brain Res*. 2009;1282:142–155.

13. Annabi B, Rojas-Sutterlin S, Laroche M, et al. The diet-derived sulforaphane inhibits matrix metalloproteinase-9-activated human brain microvascular endothelial cell migration and tubulogenesis. *Mol Nutr Food Res*. 2008;52:692–700.
14. Roomi MW, Monterrey JC, Kalinovsky T, et al. Distinct patterns of matrix metalloproteinase-2 and -9 expression in normal human cell lines. *Oncol Rep*. 2009;21:821–826.
15. Jadhav U, Chigurupati S, Lakka SS, et al. Inhibition of matrix metalloproteinase-9 reduces in vitro invasion and angiogenesis in human microvascular endothelial cells. *Int J Oncol*. 2004;25:1407–1414.
16. Verfaillie T, Garg AD, Agostinis P. Targeting ER stress induced apoptosis and inflammation in cancer. *Cancer Lett*. 2010; doi:10.1016/j.canlet.2010.07.016. In press.
17. Dong D, Ni M, Li J, et al. Critical role of the stress chaperone GRP78/BiP in tumor proliferation, survival, and tumor angiogenesis in transgene-induced mammary tumor development. *Cancer Res*. 2008; 68:498–505.
18. Stins MF, Gilles F, Kim KS. Selective expression of adhesion molecules on human brain microvascular endothelial cells. *J Neuroimmunol*. 1997; 76:81–90.
19. Greiffenberg L, Goebel W, Kim KS, et al. Interaction of Listeria monocytogenes with human brain microvascular endothelial cells: InlB-dependent invasion, long-term intracellular growth, and spread from macrophages to endothelial cells. *Infect Immun*. 1998;66: 5260–5267.
20. McLaughlin N, Annabi B, Sik Kim K, et al. The response to brain tumor-derived growth factors is altered in radioresistant human brain endothelial cells. *Cancer Biol Ther*. 2006;5:1539–1545.
21. Lamy S, Gingras D, Béliveau R. Green tea catechins inhibit vascular endothelial growth factor receptor phosphorylation. *Cancer Res*. 2002; 62:381–385.
22. Sina A, Lord-Dufour S, Annabi B. Cell-based evidence for aminopeptidase N/CD13 inhibitor actinonin targeting of MT1-MMP-mediated proMMP-2 activation. *Cancer Lett*. 2009;279:171–176.
23. Currie JC, Fortier S, Sina A, et al. MT1-MMP down-regulates the glucose 6-phosphate transporter expression in marrow stromal cells: a molecular link between pro-MMP-2 activation, chemotaxis, and cell survival. *J Biol Chem*. 2007;282:8142–8149.
24. Abécassis I, Olofsson B, Schmid M, et al. RhoA induces MMP-9 expression at CD44 lamellipodial focal complexes and promotes HMEC-1 cell invasion. *Exp Cell Res*. 2003;291:363–376.
25. Handsley MM, Edwards DR. Metalloproteinases and their inhibitors in tumor angiogenesis. *Int J Cancer*. 2005;115:849–860.
26. Noël A, Jost M, Maquoi E. Matrix metalloproteinases at cancer tumor-host interface. *Semin Cell Dev Biol*. 2008;19:52–60.
27. Dong J, Jimi E, Zeiss C, et al. Constitutively active NF-kappaB triggers systemic TNFalpha-dependent inflammation and localized TNFalpha-independent inflammatory disease. *Genes Dev*. 2010;24: 1709–1717.
28. Tahanian E, Lord-Dufour S, Das A, et al. Inhibition of tubulogenesis and of carcinogen-mediated signaling in brain endothelial cells highlight the antiangiogenic properties of a mumbaistatin analog. *Chem Biol Drug Des*. 2010;75:481–488.
29. Mertens S, Noll T, Spahr R, et al. Energetic response of coronary endothelial cells to hypoxia. *Am J Physiol*. 1990;258:H689–H694.
30. Shryock JC, Rubio R, Berne RM. Release of adenosine from pig aortic endothelial cells during hypoxia and metabolic inhibition. *Am J Physiol*. 1988;254:H223–H229.
31. Tretyakov AV, Farber HW. Endothelial cell tolerance to hypoxia. *J Clin Invest*. 1995;95:738–744.
32. Xi H, Kurtoglu M, Liu H, et al. 2-Deoxy-D: -glucose activates autophagy via endoplasmic reticulum stress rather than ATP depletion. *Cancer Chemother Pharmacol*. In press 2010.
33. Li J, Qin Z, Liang Z. The prosurvival role of autophagy in Resveratrol-induced cytotoxicity in human U251 glioma cells. *BMC Cancer*. 2009; 9:215.
34. Krmpot AJ, Janjetovic KD, Misirkic MS, et al. Protective effect of autophagy in laser-induced glioma cell death in vitro. *Lasers Surg Med*. 2010;42:338–347.
35. Nishikawa T, Tsuno NH, Okaji Y, et al. The inhibition of autophagy potentiates anti-angiogenic effects of sulforaphane by inducing apoptosis. *Angiogenesis*. 2010;13:227–238.
36. Dubois RN, Abramson SB, Crofford L, et al. Cyclooxygenase in biology and disease. *FASEB J*. 1998;12:1063–1073.
37. Antonacopoulou AG, Tsamandas AC, Petsas T, et al. EGFR, HER-2 and COX-2 levels in colorectal cancer. *Histopathology*. 2008;53: 698–706.
38. Cho HY, Thomas S, Golden EB, et al. Enhanced killing of chemo-resistant breast cancer cells via controlled aggravation of ER stress. *Cancer Lett*. 2009;282:87–97.
39. Shih RH, Yang CM. Induction of heme oxygenase-1 attenuates lipopolysaccharide-induced cyclooxygenase-2 expression in mouse brain endothelial cells. *J Neuroinflammation*. 2010;7:86.
40. Hara Y, Kuroda N, Inoue K, et al. Up-regulation of vascular endothelial growth factor expression by adenosine through adenosine A2 receptors in the rat tongue treated with endotoxin. *Arch Oral Biol*. 2009;54: 932–994.